

## Supporting Information

### **Long-life Graphite – Lithium Sulfide Full Cells Enabled through a Solvent Co-intercalation-free Electrolyte Design**

*Tianxing Lai, Amruth Bhargav, Seth Reed, and Arumugam Manthiram\**

#### **Experimental Section**

**Electrodes Preparation:** Commercial graphite (Gr) anodes (MTI Corp.) were utilized in the half cells. To prepare the Gr anodes for the full cell, Gr powder (94 wt%, MTI Corp.), super C65 (2.5 wt%), carboxymethyl cellulose (CMC, 1.75 wt%), and styrene–butadiene–rubber (SBR, 1.75 wt%) were mixed in water with 0.1 wt.% of the oxalic acid additive in a Thinky mixer. The CMC-SBR was pre-dissolved in water to make a 1.5 wt% solution. The slurry was then cast onto a copper foil and dried under vacuum. The electrodes were then punched into 9/16-in. round disks before use. The N/P ratio was calculated based on the theoretical capacities of Gr (330 mA h g<sup>-1</sup>), sulfur (1,672 mA h g<sup>-1</sup>), and Li<sub>2</sub>S (1,165 mA h g<sup>-1</sup>).

Silicon-graphite (Si-Gr) anodes were prepared by a slurry blade-cast method. Si-Gr powder (80 wt%, Canrd), super C65 (10 wt%), and CMC-SBR (10 wt%) were mixed in water in a Thinky mixer. The slurry was then cast onto a copper foil and dried under vacuum. The electrodes were then punched into 9/16-in. round disks before use.

Li<sub>2</sub>S cathodes were prepared by a slurry blade-cast method. A 4 wt% binder solution of polyethylene oxide (PEO, average MW ≈ 4,000,000, Sigma Aldrich) and polyvinylpyrrolidone (PVP, average MW ≈ 1,300,000, Ashland) (w/w = 4:1) was prepared in acetonitrile. Li<sub>2</sub>S (70 wt%,

Thermo Scientific), carbon nanofiber (CNF, 10 wt%, XFNANO), super C65 (10 wt%), and PEO/PVP binder solution (10 wt% of solid) were mixed in a plastic bottle by a roll jar-milling system for 48 h at 70 rpm. DME and 1,4-dioxane were added to control the overall solid content at 15–17 wt%. 5 and 8 mm yttria-stabilized zirconia (YSZ) grinding balls (Advanced Materials) were used to as the milling media. The slurry was then doctor-blade cast onto carbon-coated aluminum foil inside an Ar-filled glovebox and dried under vacuum overnight. The electrodes were punched into 7/16-in. diameter disks before use.

To prepare the sulfur/Ketjen Black (KB) composite for the sulfur cathodes, sulfur powder (75 wt%, ~100 mesh, Thermo Scientific) and KB (25 wt%, EC-600JD) were ground and melt diffused in an autoclave at 155 °C for 12 h. The S/KB composite (80 wt%), super C65 (5 wt%), carbon nanofibers (CNF, 5 wt%), and PEO/PVP binder solution (10 wt% of solid) were mixed in water in a Thinky mixer. The slurry was then doctor-blade cast onto carbon-coated aluminum foil and then dried at 50 °C under vacuum overnight. The electrodes were punched into 7/16-in. diameter disks before use.

**Electrolyte Preparation:** The control electrolyte was composed of 1 M lithium bis(trifluoromethanesulfonyl)imide (LiTFSI, Solvionic) and 0.25 M LiNO<sub>3</sub> in 1,3-dioxolane (DOL) and 1,2-dimethoxyethane (DME) (v/v = 1:1). DOL/TTE electrolyte was prepared by dissolving 1 M LiTFSI in DOL and 1,1,2,2-tetrafluoroethyl 2,2,3,3-tetrafluoropropyl ether (TTE) (v/v = 1:1).

**Electrochemical Measurements:** All coin cells were assembled with CR2032 cell cases inside an Ar-filled glovebox. One layer of Celgard 2325 separator was utilized in each cell. 40 μL of electrolyte was added in the Li || Gr and Li || Si-Gr half cells. An electrolyte-to-sulfur (E/S) ratio

of 10 was applied for sulfur and  $\text{Li}_2\text{S}$  cells. The cells were rested for 5 h before being cycled at 21 °C. For  $\text{Li} \parallel \text{Gr}$  cells, galvanostatic cycling tests were performed at a rate of  $C/10$  for one formation cycle and then at  $C/5$  rate between 0.005 and 1.5 V. For  $\text{Li} \parallel \text{Si-Gr}$  cells, cycling tests were performed at  $C/2$  rate between 0.005 and 1.2 V after one formation cycle at  $C/5$  rate. For lithiated- $\text{Gr} (\text{Li-Gr}) \parallel \text{S}$  cells, they were activated at  $C/20$  rate for 10 cycles before cycling at  $C/10$  rate between 1.5 and 2.8 V. For  $\text{Gr} \parallel \text{Li}_2\text{S}$  cells, they were activated at  $C/30$  rate for 1 cycle and then cycled at  $C/10$  rate between 1.5 and 3 V. All the cycling data were collected on a Landt or an Arbin cyler. Cyclic voltammetry (CV) tests were conducted in the potential range of 0.005 to 1.5 V for  $\text{Li} \parallel \text{Gr}$  cells with a scan rate of  $0.05 \text{ mV s}^{-1}$ . Electrochemical impedance spectroscopy (EIS) measurements were performed in the frequency range of 1 MHz to 0.05 Hz. CV and EIS data were collected on a Biologic VMP-3 system.

**Materials Characterization:** Operando X-ray diffraction (XRD) analysis was carried out on a Rigaku Ultima IV X-ray diffractometer with a specially designed cell (MTI Corp). Raman spectra were collected with a Renishaw Raman spectrometer. A PHI VersaProbe 4 X-ray photoelectron spectrometer was used for XPS analysis. The cycled Li samples were sputtered for various amounts of time with Ar clusters. Online electrochemical mass spectrometry (OEMS) measurements were conducted to understand the anode outgassing behavior. The details of the setup of the OEMS system can be found in our previous publication.<sup>1</sup> A commercial cell (PAT-Cell-Gas, EL-CELL) was assembled with Gr, Li metal, and different electrolytes for the measurement. The cell was rested for 9 h, followed by a  $C/10$  discharge to 0.005 V and a constant-voltage hold at 0.005 V. The experiment was carried out in a 30 °C temperature chamber.

**Computational methods:** Classical molecular dynamics (MD) simulations were performed with the GROMACS 2024 software package.<sup>2,3</sup> OPLS-AA force field was chosen for the simulations.<sup>4</sup> 1.2\*CM5 charge model was applied to the solvent molecules, while parameters from 0.8\*OPLS-2009IL force field were derived for TFSI<sup>-</sup> and NO<sub>3</sub><sup>-</sup>.<sup>5</sup> The simulation cell of the DOL/TTE electrolyte consists of 703 DOL, 326 TTE, and 98 LiTFSI, while the DME/DOL cell contains 660 DOL, 444 DME, 92 LiTFSI, and 23 LiNO<sub>3</sub>. The initial coordinates of the molecules were generated by the Packmol program in a 6 × 6 × 6 nm<sup>3</sup> simulation box. First, an energy minimization was performed for each system with the conjugate gradient method. Then, an annealing process was performed with NPT ensemble (at 1 bar) to ensure the equilibrium of the system, including heating from 0 to 330 K in 1 ns, holding at 330 K for 4 ns, and cooling to 298 K, followed by 4 ns running at 298 K. In the process, a timestep of 1 fs was used. The C-rescale barostat and V-rescale thermostat were used to control the pressure and temperature, respectively. Last, 5 ns of NPT production run was performed to analyze the structure of the electrolyte.

Density functional theory (DFT) calculations were performed with the Gaussian 16 software package.<sup>5</sup> B3LYP-GD3(BJ) functional and the 6-311+G(d, p) basis set were used for structure optimization of solvent molecules (for MD simulations) and solvation structures obtained from the MD results.<sup>7</sup> M06-2X functional and the ma-def2-TZVP basis set were used for single point energy calculations.<sup>8</sup> The IEFPCM implicit solvation model was applied to describe the solvent effect. The binding energy between a solvent molecule and the solvation structure was calculated by the following equation:

$$E_{binding} = E_{total} - E_{solvent} - E_{remain}$$

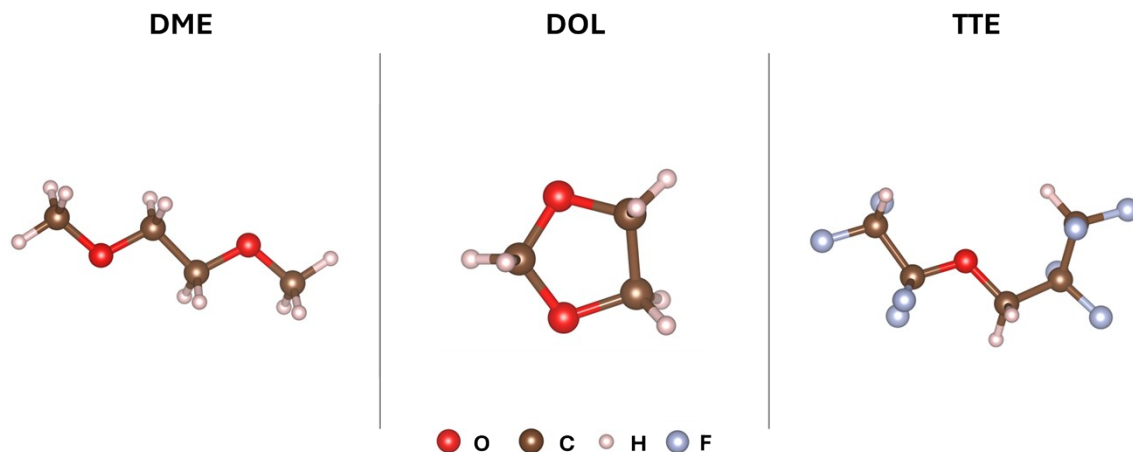


**Fig. S1.** Molecular structures of DME, DOL, and TTE.

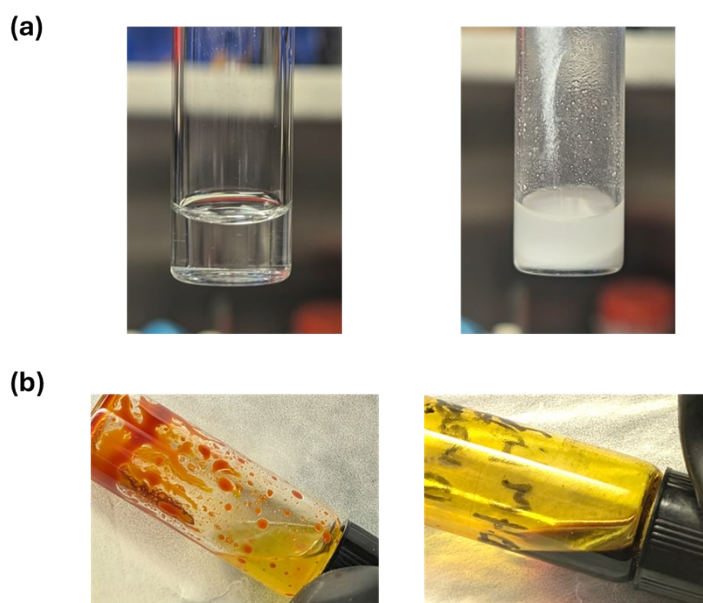


**Fig. S2.** (a) Solubility test of 1 M LiTFSI in DME (left) and TTE (right). (b) Digital photos of 0.2 M  $\text{Li}_2\text{S}_6$  in DOL/TTE mixture (left) and DOL/DME mixture (right). From the color difference of the solutions and the precipitation, we can see that the DOL/TTE system has a much lower solubility for polysulfides.

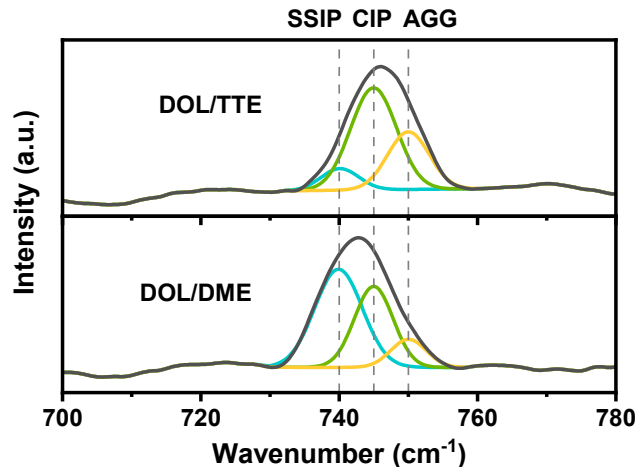


**Fig. S3.** Raman spectra of the DOL/TTE and DOL/DME electrolytes. Based on the area of each S-N-S vibration peak, there are 10.3 % solvation separated ion pairs (SSIPs), 59.4% contact-ion pairs (CIPs), and 30.3% aggregates (AGGs) in the DOL/TTE electrolyte, while 53.2% SSIPs, 35.6% CIPs, and 11.3% AGGs in the DOL/DME electrolyte.

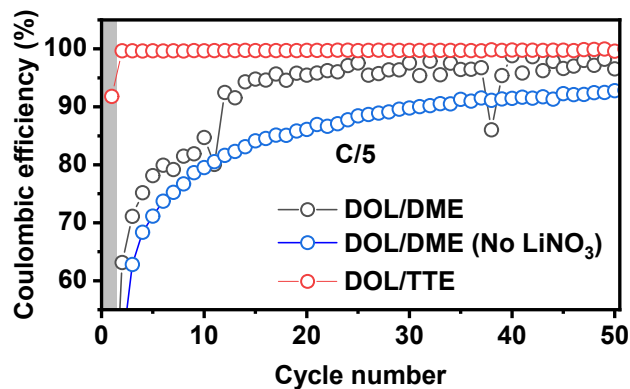


**Fig. S4.** Coulombic efficiency of Li || Gr cells with the DOL/DME (with and without LiNO<sub>3</sub>) and DOL/TTE electrolytes.

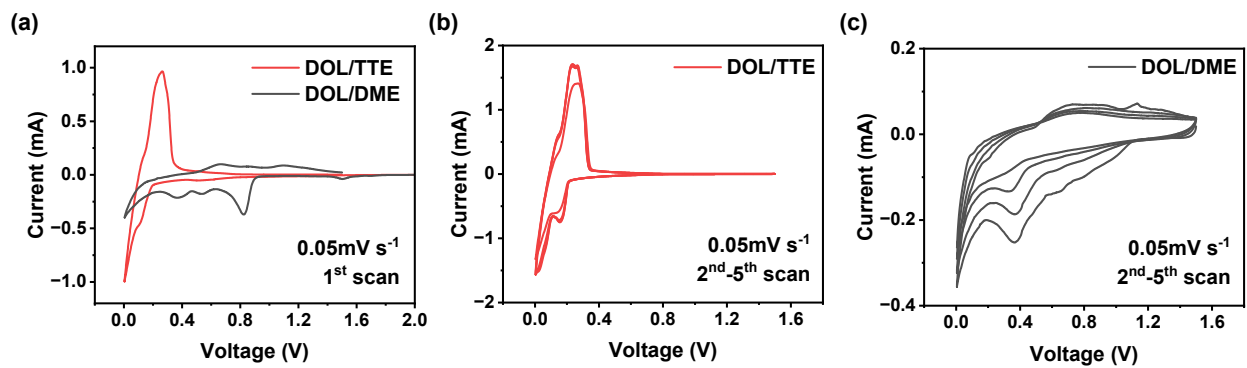


Fig. S5. CV curves of Gr || Li cells with the DOL/TTE and DOL/DME electrolytes.

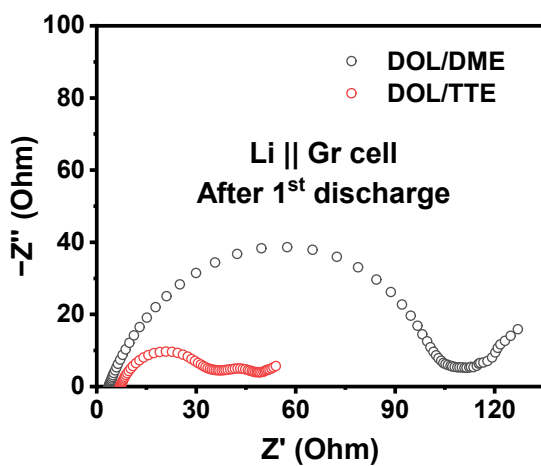
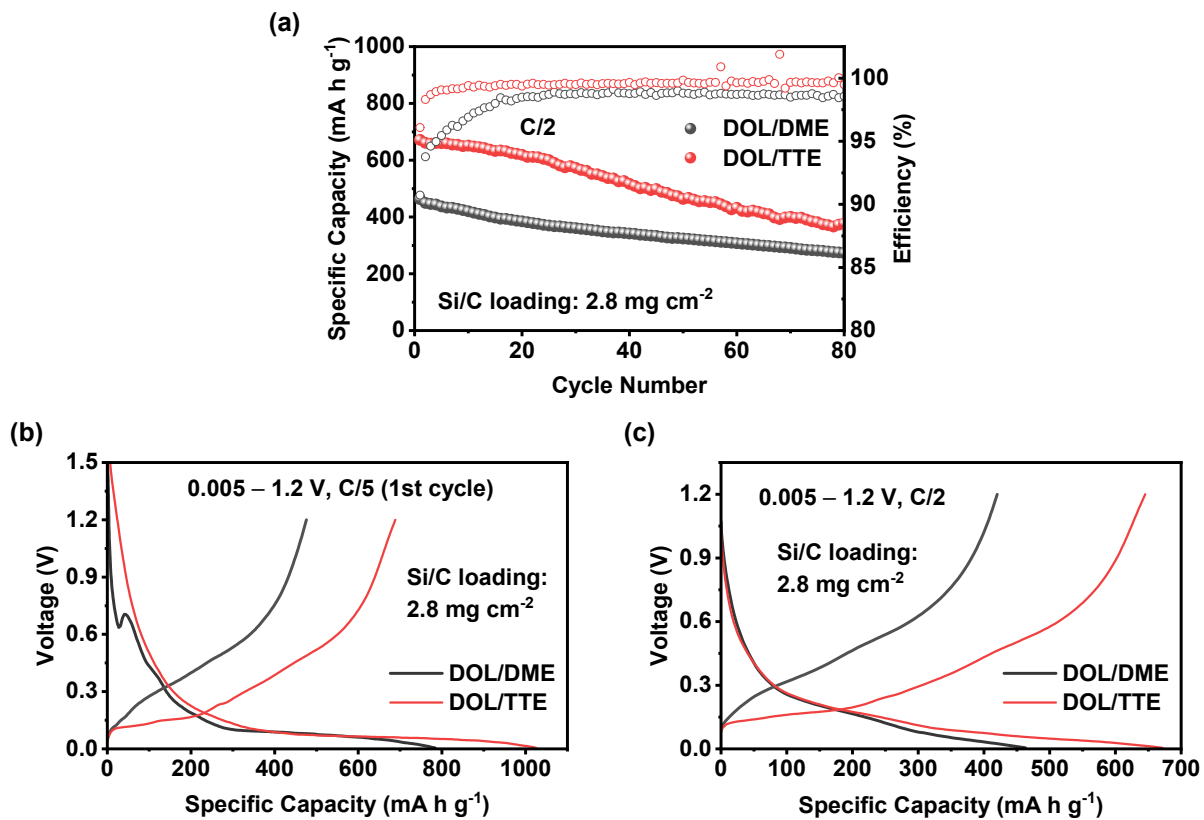
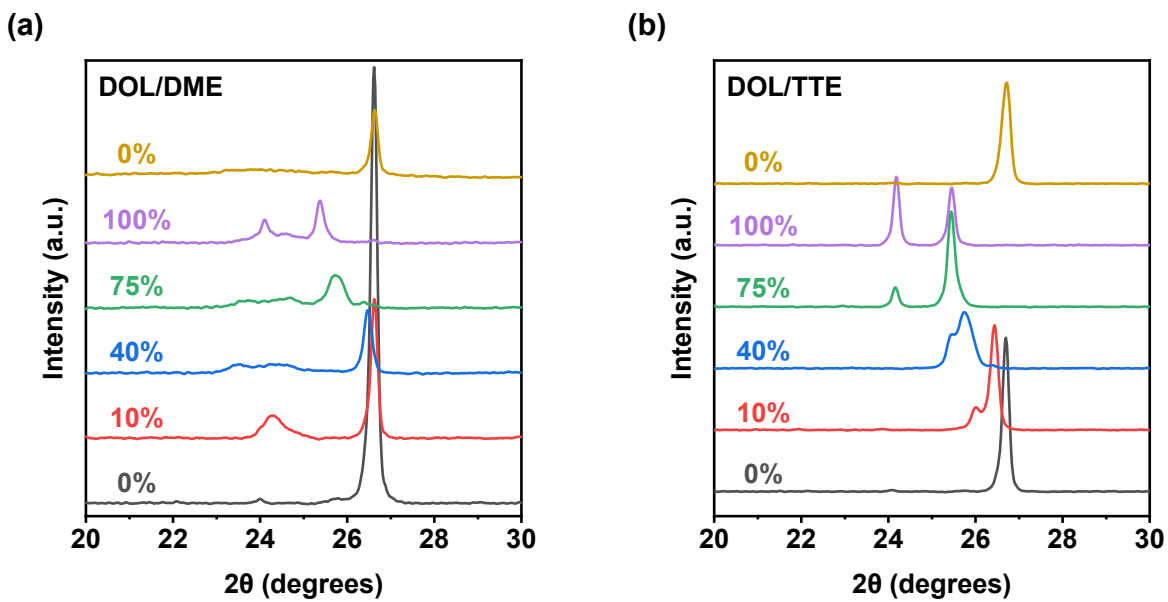


Fig. S6. Nyquist plots of Li || Gr cells after one discharge process in different electrolytes.



**Fig. S7.** (a) Cycling performance of Li || Si/C cells in different electrolytes, and the corresponding voltage profiles of the (b) formation cycle at C/5 rate and (c) the 1<sup>st</sup> cycle at C/2 rate.





**Fig. S8.** Selected operando XRD patterns of Gr anodes at different discharged states in (a) the DOL/TTE and (b) DOL/DME electrolytes.

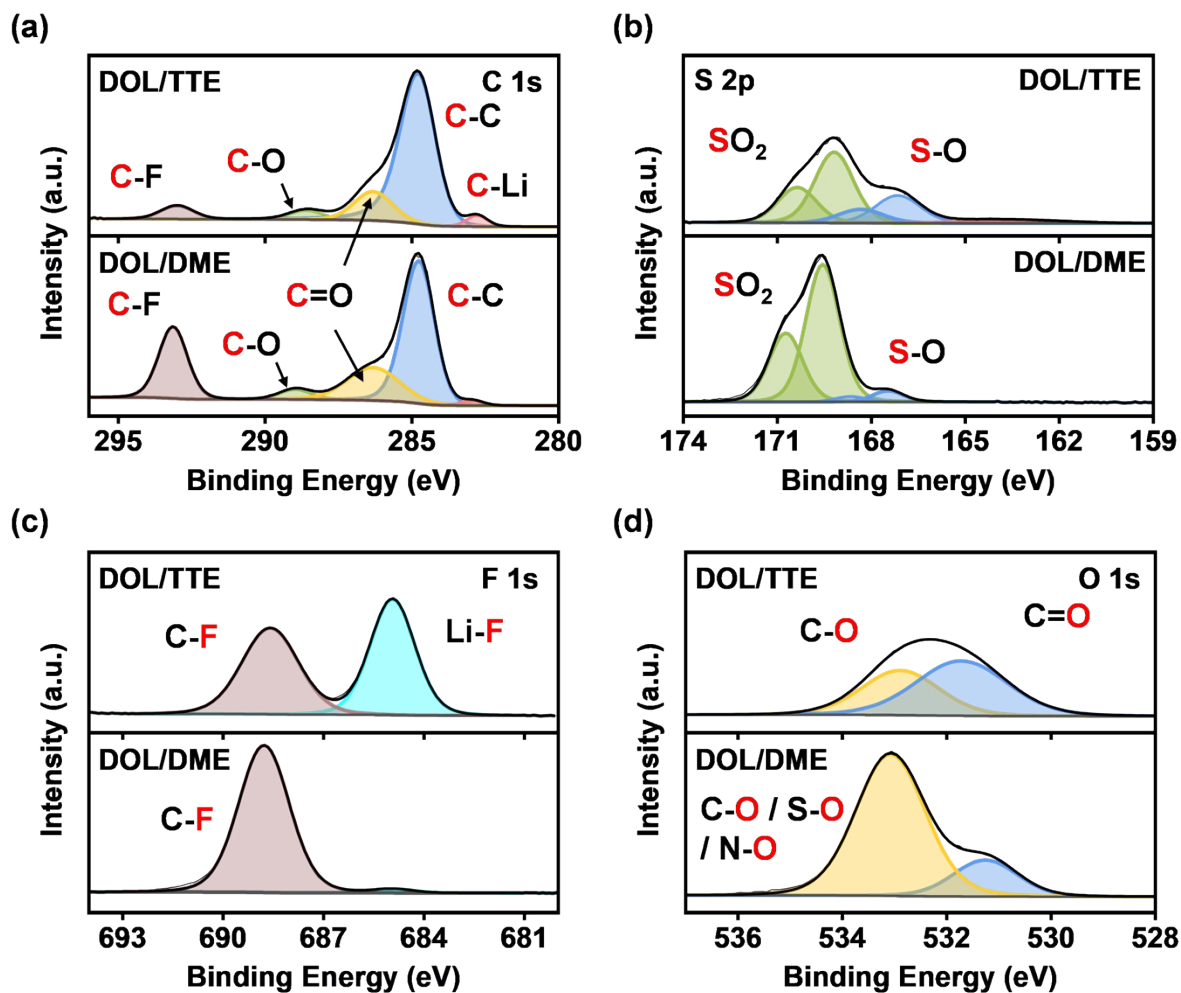


**Fig. S9.** (a) C 1s, (b) S 2p, (c) F 1s, and (d) O 1s XPS data of the cycled Gr anodes in Gr || Li cells with the DOL/TTE and DOL/DME electrolytes.

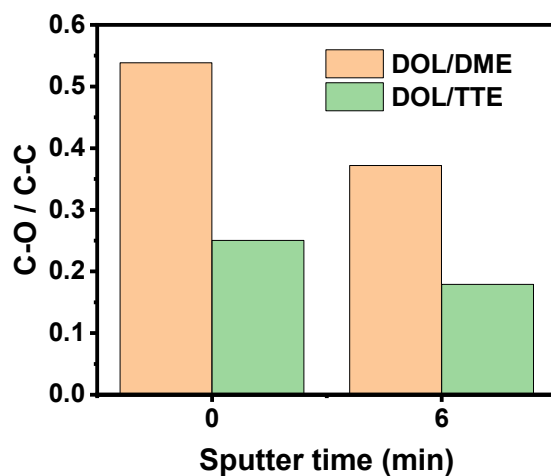


**Fig. S10.** Ratios between C-O (including both C-O and C=O) and C-C bonding from the C 1s spectra before and after 6 min of sputtering.

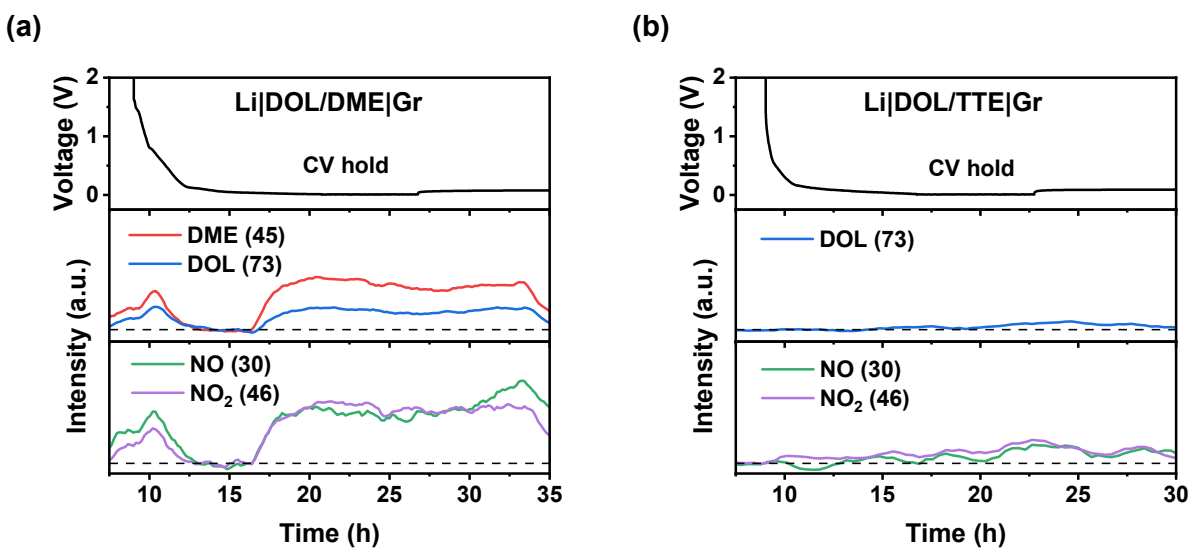


**Fig. S11.** Voltage profiles (top) and the corresponding gas generation plots (bottom) for Li || Gr cells with (a) the DOL/TTE and (b) DOL/DME electrolytes.

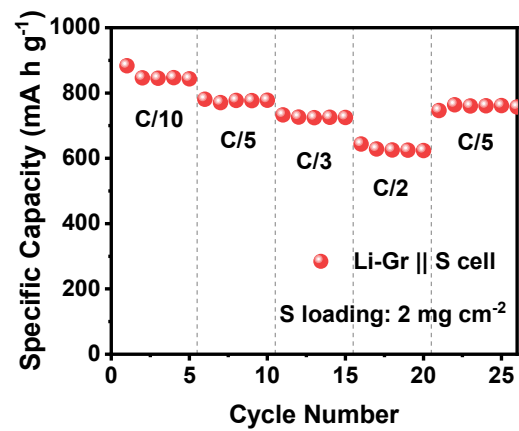


**Fig. S12.** Rate performance of Li || S cells with the DOL/TTE electrolyte.

## References

- 1 J. Langdon, R. Sim and A. Manthiram, *ACS Energy Lett.*, 2022, **7**, 2634-2640.
- 2 M. J. Abraham, T. Murtola, R. Schulz, S. Páll, J. C. Smith, B. Hess and E. Lindahl, *SoftwareX*, 2015, **1-2**, 19-25.
- 3 D. Van Der Spoel, E. Lindahl, B. Hess, G. Groenhof, A. E. Mark and H. J. Berendsen, *J. Comput. Chem.*, 2005, **26**, 1701-1718.
- 4 W. L. Jorgensen, D. S. Maxwell and J. TiradoRives, *J. Am. Chem. Soc.*, 1996, **118**, 11225-11236.
- 5 B. Doherty, X. Zhong, S. Gathiaka, B. Li and O. Acevedo, *J. Chem. Theory Comput.*, 2017, **13**, 6131-6145.
- 6 Gaussian 16, Revision C.01, 2016, Gaussian, Inc. Wallingford CT.
- 7 P. J. STEPHENS, F. J. DEVLIN, C. F. CHABALOWSKI and M. J. FRISCH, *Journal of Physical Chemistry*, 1994, **98**, 11623-11627.
- 8 Y. Zhao and D. G. Truhlar, *Theor. Chem. Acc.*, 2008, **120**, 215-241.